

Formation of quantum dots in GaN/AlGaN FETs

Tomohiro Otsuka,^{1,2,3,4,*} Takaya Abe,¹ Takahito Kitada,¹

Norikazu Ito,⁵ Taketoshi Tanaka,⁵ and Ken Nakahara⁵

¹*Research Institute of Electrical Communication, Tohoku University,
2-1-1 Katahira, Aoba-ku, Sendai 980-8577, Japan*

²*Center for Spintronics Research Network, Tohoku University,
2-1-1 Katahira, Aoba-ku, Sendai 980-8577, Japan*

³*Center for Science and Innovation in Spintronics,
Tohoku University, 2-1-1 Katahira, Aoba-ku, Sendai 980-8577, Japan*

⁴*Center for Emergent Matter Science, RIKEN,
2-1 Hirosawa, Wako, Saitama 351-0198, Japan*

⁵*ROHM Co., Ltd, 21 Saiinnmizosakicho,
Ukyo-ku, Kyoto, Kyoto 615-8585, Japan*

(Dated: May 20, 2020)

Abstract

GaN and the heterostructures are attractive in condensed matter science and applications for electronic devices. We measure the electron transport in GaN/AlGaN field-effect transistors (FETs) at cryogenic temperature. We observe formation of quantum dots in the conduction channel near the depletion of the 2-dimensional electron gas (2DEG). Multiple quantum dots are formed in the disordered potential induced by impurities in the FET conduction channel. We also measure the gate insulator dependence of the transport properties. These results can be utilized for the development of quantum dot devices utilizing GaN/AlGaN heterostructures and evaluation of the impurities in GaN/AlGaN FET channels.

GaN and the heterostructures are attractive materials because of their interesting electronic properties: the large direct bandgap, the high electron densities and mobilities. They are utilized in light-emitting diodes [1–3], power and high-frequency electronics devices [4–6]. In electronic device applications, GaN/AlGaIn heterostructures are important structures. High density and high mobility 2DEG is formed at the interface [7, 8]. The 2DEG is also investigated on the view-point of spin-orbit interactions [9–11] and electron spin resonances [12]. Quantum nanostructures can be fabricated from the heterostructure by utilizing nano-fabrications. Quantum point contacts [13] and single electron transistors [14] are reported. GaN/AlGaIn nanowires [15, 16] and self-assembled GaN islands [17] are also used to form quantum dots. Then GaN and the heterostructures are attractive also in quantum devices utilizing the electronic properties.

Quantum dots can be formed also by intrinsic impurity potentials not only by the electric gates or edges defined structures. In Si FETs, the formation of quantum dots by electrical potentials induced by dopants is reported [18–20]. Dopants themselves work as quantum dots and control of the dopants [21] is used for quantum bit applications [22–26], which is studied for quantum information processing [27, 28]. The stronger confinement by the dopant makes larger quantization energies and this enables high-temperature operation of the semiconductor quantum bits [29].

In this paper, we measure electron transport through GaN/AlGaIn FETs at cryogenic temperature. We observe non-monotonic modulation of the current indicating formation of quantum dots near the pinch-off condition of the FET channel. Multiple quantum dots are formed in the potential fluctuations induced by the impurities near the conduction channel. We also measure the gate insulator dependence.

RESULTS

Device and FET properties

Figure 1(a) shows a schematic of the layer structure of the device. GaN and AlGaIn layer is grown on the Si substrate by chemical vapor deposition. At the interface between the GaN and AlGaIn layers, 2DEG is formed. The typical values of the electron density and the mobility are $6.7 \times 10^{12} \text{ cm}^{-2}$ and $1700 \text{ cm}^2 \text{ V}^{-1} \text{ s}^{-1}$. Source and drain contacts are prepared by Ti/Al. A TiN gate electrode is deposited on the insulator of SiN and SiO₂. SiN is grown in-situ just after the growth of the GaN/AlGaIn. An optical image of the device is Fig. 1(b). The gate electrode is

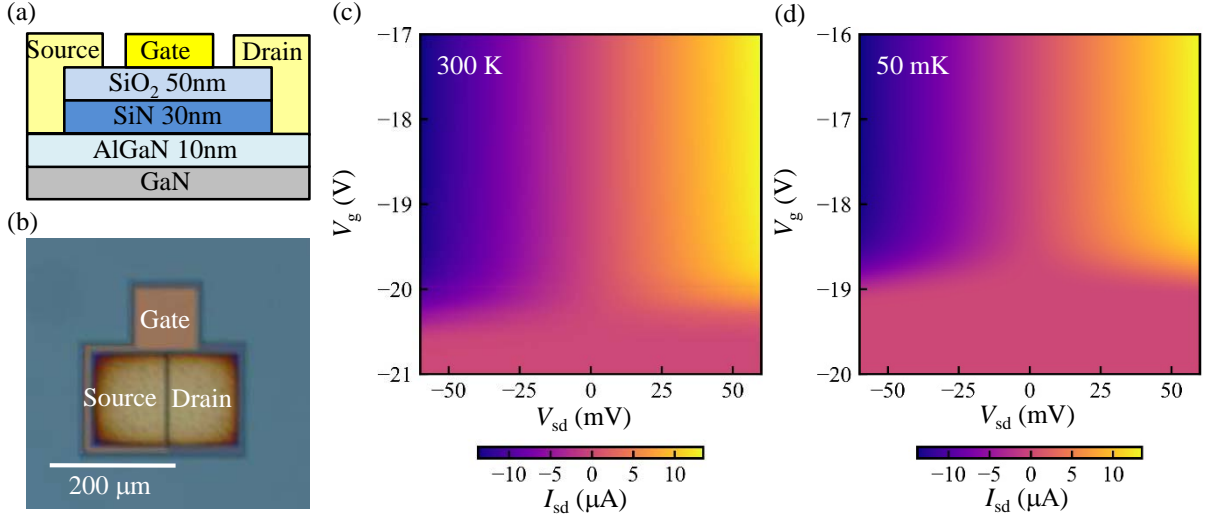


FIG. 1. (a) Schematic of the layer structure of the device. 2 DEG is formed at the interface between GaN and AlGaIn. (b) Optical image of the device. The gate electrode with $1.4 \mu\text{m}$ gate length is placed between the source and the drain. (c), (d) Current trough the GaN/AlGaIn FET as a function of the source-drain bias voltage V_{sd} and the gate voltage V_{g} at 300 K (c) and 50 mK (d).

placed between the source and the drain contacts. The gate length and the gate width are $1.4 \mu\text{m}$ and $150 \mu\text{m}$, respectively.

The current between the source and the drain contacts I_{sd} is measured as a function of the applied source-drain bias voltage V_{sd} and the gate voltage V_{g} . We measure the current through the device at the room temperature 300 K and cryogenic temperature 50 mK. The device is cooled down by a dilution refrigerator.

Figure 1(c) shows the measured current through the GaN/AlGaIn FET I_{sd} at the room temperature 300 K. In $V_{\text{g}} > -20.5 \text{ V}$, the FET channel is opened and the current flows depending on V_{sd} . In the measurement, two $1 \text{ k}\Omega$ resistors, which is used for low pass filters designed for the cryogenic measurement, are inserted in series to the device and this limits the current in the open condition of the FET. Around $V_{\text{g}} \sim -20.5 \text{ V}$, the conduction channel is depleted. No current flows in more negatively gated region $V_{\text{g}} < -20.5 \text{ V}$.

Figure 1(d) shows the measured I_{sd} at the cryogenic temperature 50 mK. The conduction channel remains at this temperature in $V_{\text{g}} > -19 \text{ V}$. The depletion of the conduction channel occurs around $V_{\text{g}} \sim -19 \text{ V}$. The pinch-off voltage shifts 1.5 V positively compared to the result at the room temperature. This is induced by the suppression of the thermally induced carriers at the

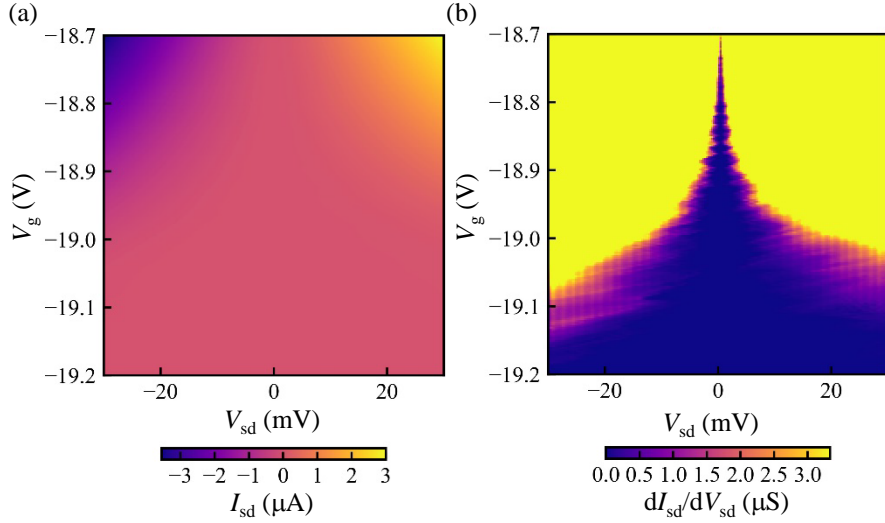


FIG. 2. (a) Current through the FET as a function of the source-drain bias voltage V_{sd} and the gate voltage V_g at 50 mK near the depletion condition of the 2DEG. (b) The numerical derivative of the measured current as a function of the source-drain bias voltage dI_{sd}/dV_{sd} . Non-monotonic modulation of the current and Coulomb diamond structures are observed.

cryogenic temperature.

Formation of quantum dots

Figure 2(a) shows the current through the FET near the depletion condition of the 2DEG. The current is suppressed around the zero bias and non-linear I-V properties are observed in this region. A numerical derivative of the measured current as a function of the source-drain bias voltage dI_{sd}/dV_{sd} is shown in Fig. 2(b). The current I_{sd} is blocked around the zero bias condition $V_{sd} \sim 0$. The width of the blocked region is modulated by the gate voltage V_g and Coulomb diamonds are observed. The size of the diamonds becomes larger in more negative values of V_g and this reflects that the dot size becomes smaller and the charging energy becomes larger. Note that the faint vertical lines around the outside of the diamonds are the measurement artifact that originates from the output voltages of the source measure unit used in this measurement.

Figure 3(a) shows the closed up image of the Coulomb diamonds. In this small current condition, we use a current preamplifier to measure the current instead of the source measure unit and the measurement artifact like in Fig. 2(b) is not there. The current enhancement by the excited

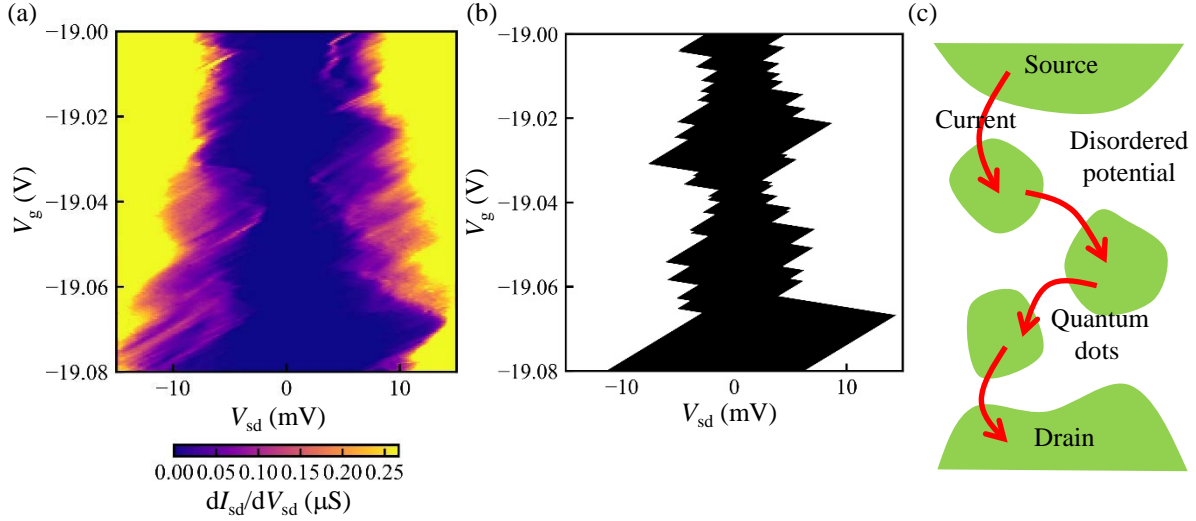


FIG. 3. (a) Numerical derivative of the current as a function of the source-drain bias voltage. Coulomb diamonds are observed. (b), (c) Schematic of the one possible configuration of the quantum dots (c) and the expected Coulomb diamonds (b). Electrostatic potential will be disordered by the impurities and defects and the quantum dots are formed at the potential minima. Here we assumed that three quantum dots coupled in series and the overlapped Coulomb diamonds show gaps around the zero bias conditions.

states is also observed as lines outside of the Coulomb diamonds. Quantum dots are formed in the conduction channel of the FET.

The visible lines mostly have the same slope and this indicates that the dot is asymmetrically coupled to the leads: the dot is strongly coupled to one of the leads. The voltage drop by forming the large in-series resistance in the conduction channel is negligible, which can be evaluated by inverting the source and the drain contacts in the measurement [30]. The diamonds are not completely closed at $V_{sd} = 0$ in Fig. 3(a). This shows that multiple quantum dots are formed in this device.

DISCUSSION

There are no small fine gates or structures to define quantum dots intentionally in this device. The quantum dots will be formed by the disordered potential induced by the impurities or defects near the conduction channel. Near the depletion of the 2DEG, the potential minima of the disordered potential contribute to the transport and coupled quantum dots are formed.

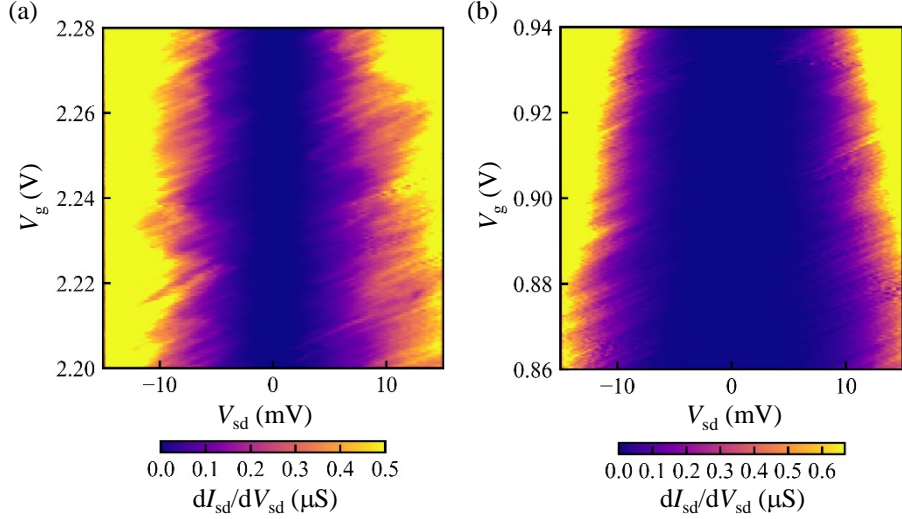


FIG. 4. (a), (b) Numerical derivative of the current as a function of the source-drain bias voltage observed in other samples with different insulators SiO₂ (a) and SiN/SiO₂.

Figure 3(c) is a schematic of one possible configuration of the formed quantum dots. Three quantum dots are coupled in series. The resulting Coulomb diamonds become the overlap of the diamonds of each dot in a simple approximation [31]. Figure 3(b) shows the result when we assume the three quantum dots with charging energies $E_{C1}, E_{C2}, E_{C3} = 2.6, 2.3, 3.0$ meV, orbital level spacing $\Delta\epsilon_1, \Delta\epsilon_2, \Delta\epsilon_3 = 0.97 - 11, 0.81 - 4.1, 0.65 - 2.9$ meV and alfa factor $\alpha = 0.0079$. The black area indicates the Coulomb blocked region. The model capture the main feature of Fig. 3(a).

To study the growth condition dependence of the quantum dot formation, we measure other samples with different gate insulators and fabrication processes, which induce different disorder densities. In these new samples, the insulator is fabricated after taking out the samples from the growth chamber of GaN/AlGa_N and etching processes. The gate length is $0.6 \mu\text{m}$. Higher disorder densities are expected compared to the previous sample which has SiN insulators grown in-situ in the same chamber. Figure 4(a) and (b) show the results measured in devices with SiO₂ and SiN/SiO₂ insulators, respectively. Compared to Fig. 3(a), more Coulomb diamonds are overlapped and the larger opening of the gap around the zero bias condition is observed. More quantum dots are formed and coupled in series. This is consistent with the expectation that the higher disorder density forms more quantum dots in these devices. These support that the origin of the formation of the quantum dots is the disordered potentials around the FET channels.

In conclusion, we measure electron transport in GaN/AlGaN FETs at cryogenic temperature. Quantum dots are formed in the conduction channel near the depletion of the 2DEG. Multiple quantum dots are formed by the disordered potential in the FET. We also measured insulator dependence of the quantum dot formation. These results can be utilized for the development of quantum dot devices like semiconductor quantum bits and nano-probes [32–34] utilizing GaN/AlGaN and evaluation of the disordered potential in GaN/AlGaN FET channels.

ACKNOWLEDGEMENTS

We thank Takeshi Kumasaka for fruitful discussions and technical supports. Part of this work is supported by ROHM Collaboration Project, PRESTO (JPMJPR16N3), JST, Futaba Electronics Memorial Foundation Research Grant, Iketani Science and Technology Foundation Research Grant, Yamaguchi Foundation Research Grant, The Mikiya Science and Technology Foundation Research Grant, Harmonic Ito Foundation Research Grant, Takahashi Industrial and Economic Research Foundation Research Grant, The Murata Science Foundation Research Grant, Samco Foundation Research Grant, Casio Science Promotion Foundation Research Grant.

AUTHOR CONTRIBUTIONS

T. O. and K. N. planned the project; N. I., T. T., and K. N. performed device fabrication; T. O., T. A., T. K., N. I., T. T., and K. N. conducted experiments and data analysis; all authors discussed the results; T. O., T. A., T. K., T. T., and K. N. wrote the manuscript.

ADDITIONAL INFORMATION

Competing financial interests: The authors declare no competing financial interests.

* tomohiro.otsuka@riec.tohoku.ac.jp

[1] Akasaki, I. & Amano, H. Widegap Column-III Nitride Semiconductors for UV/Blue Light Emitting Devices. *J. Electrochem. Soc.* 141, 2266-2271 (1994).

[2] Nakamura, S. & Fasol, G. *The blue laser diode.* (Springer, Berlin, 1997).

- [3] Akasaki, I. Fascinating journeys into blue light (Nobel Lecture). *Ann. Phys.* 527, 311-326 (2015).
- [4] Mishra, U. K., Parikh, P. & Wu, Y. F. AlGa_N/Ga_N HEMTs - An overview of device operation and applications. *Proc. IEEE* 90, 1022-1031 (2002).
- [5] Ikeda, N. et al. Ga_N power transistors on si substrates for switching applications. *Proc. IEEE* 98, 1151-1161 (2010).
- [6] Baliga, B. J. Gallium nitride devices for power electronic applications. *Semicond. Sci. Technol.* 28, 074011-1-8 (2013).
- [7] Ambacher, O. et al. Two-dimensional electron gases induced by spontaneous and piezoelectric polarization charges in N- And Ga-face AlGa_N/Ga_N heterostructures. *J. Appl. Phys.* 85, 3222-3233 (1999).
- [8] Manfra, M. J. et al. Electron mobility exceeding 160000 cm²/V s in AlGa_N/Ga_N heterostructures grown by molecular-beam epitaxy. *Appl. Phys. Lett.* 85, 5394-5396 (2004).
- [9] Thillozen, N. et al. Weak antilocalization in gate-controlled Al_x Ga_{1-x} N Ga_N two-dimensional electron gases. *Phys. Rev. B* 73, 241311-1-4 (2006).
- [10] Schmult, S. et al. Large Bychkov-Rashba spin-orbit coupling in high-mobility Ga_N Al_x Ga_{1-x} N heterostructures. *Phys. Rev. B* 74, 033302-1-4 (2006).
- [11] Kurdak, C., Biyikli, N., Ozgur, U., Morkoc, H. & Litvinov, V. I. Weak antilocalization and zero-field electron spin splitting in Al_x Ga_{1-x} N AlN Ga_N heterostructures with a polarization-induced two-dimensional electron gas. *Phys. Rev. B* 74, 113308-1-4 (2006).
- [12] Shchepetilnikov, A. V. et al. Electron spin resonance in a 2D system at a Ga_N/AlGa_N heterojunction. *Appl. Phys. Lett.* 113, 052102-1-3 (2018).
- [13] Chou, H. T. et al. High-quality quantum point contacts in Ga_NAlGa_N heterostructures. *Appl. Phys. Lett.* 86, 073108-1-3 (2005).
- [14] Chou, H. T. et al. Single-electron transistors in Ga_N/AlGa_N heterostructures. *Appl. Phys. Lett.* 89, 033104-1-3 (2006).
- [15] Ristić, J. et al. Columnar AlGa_N/Ga_N nanocavities with AlN/Ga_N bragg reflectors grown by molecular beam epitaxy on Si(111). *Phys. Rev. Lett.* 94, 146102-1-4 (2005).
- [16] Songmuang, R. et al. Quantum transport in Ga_N/AlN double-barrier heterostructure nanowires. *Nano Lett.* 10, 3545-3550 (2010).
- [17] Nakaoka, T., Kako, S., Arakawa, Y. & Tarucha, S. Coulomb blockade in a self-assembled Ga_N quantum dot. *Appl. Phys. Lett.* 90, 162109-1-3 (2007).

- [18] Sellier, H. et al. Transport spectroscopy of a single dopant in a gated silicon nanowire. *Phys. Rev. Lett.* 97, 206805-1-4 (2006).
- [19] Ono, Y. et al. Conductance modulation by individual acceptors in Si nanoscale field-effect transistors. *Appl. Phys. Lett.* 90, 102106-1-3 (2007).
- [20] Tabe, M. et al. Single-Electron Transport through Single Dopants in a Dopant-Rich Environment. *Phys. Rev. Lett.* 105, 016803-1-4 (2010).
- [21] Tan, K. Y. et al. Transport Spectroscopy of single phosphorus donors in a silicon nanoscale transistor. *Nano Lett.* 10, 11-15 (2010).
- [22] Loss, D., DiVincenzo, D. P. & DiVincenzo, P. Quantum computation with quantum dots. *Phys. Rev. A* 57, 120-126 (1997).
- [23] Koppens, F. H. L. et al. Driven coherent oscillations of a single electron spin in a quantum dot. *Nature* 442, 766-771 (2006).
- [24] Yoneda, J. et al. Fast electrical control of single electron spins in Quantum dots with vanishing influence from nuclear spins. *Phys. Rev. Lett.* 113, 267601-1-5 (2014).
- [25] Veldhorst, M. et al. A two-qubit logic gate in silicon. *Nature* 526, 410-414 (2015).
- [26] Yoneda, J. et al. A quantum-dot spin qubit with coherence limited by charge noise and fidelity higher than 99.9%. *Nat. Nanotechnol.* 13, 102-106 (2018).
- [27] Nielsen, M. A. & Chuang, I. L. *Quantum Computation and Quantum Information.* (Cambridge University Press, 2000). 7.
- [28] Ladd, T. D. et al. Quantum computers. *Nature* 464, 45-53 (2010).
- [29] Ono, K., Mori, T. & Moriyama, S. High-temperature operation of a silicon qubit. *Sci. Rep.* 9, 469-1-8 (2019).
- [30] Ono K., Tanamoto T. & Ohguro T. Pseudosymmetric bias and correct estimation of Coulomb/confinement energy for unintentional quantum dot in channel of metal-oxide-semiconductor field-effect transistor. *Appl. Phys. Lett.* 103, 183107-1-4 (2013).
- [31] Nuryadi, R., Ikeda, H., Ishikawa, Y. & Tabe, M. Ambipolar Coulomb blockade characteristics in a two-dimensional Si multidot device. *IEEE Trans. Nanotechnol.* 2, 231235 (2003).
- [32] Altimiras, C. et al. Tuning energy relaxation along quantum hall channels. *Phys. Rev. Lett.* 105, 226804-1-4 (2010).
- [33] Otsuka, T. et al. Higher-order spin and charge dynamics in a quantum dot-lead hybrid system. *Sci. Rep.* 7, 12201-1-7 (2017).

- [34] Otsuka, T. et al. Difference in charge and spin dynamics in a quantum dot-lead coupled system. *Phys. Rev. B* 99, 085402-1-5 (2019).